Effect of Horizontal AC Electric Field on the Stability of Natural Convection in a Vertical Dielectric Fluid Layer

B. M. Shankar[1†], J. Kumar[2], I. S. Shivakumara[3] and S. B. Naveen Kumar[1]

[1]Department of Mathematics, PES University, Bangalore 560 085, India.
[2]ISRO Satellite Centre, Bangalore 560 017, India
[3]Department of Mathematics, Bangalore University, Bangalore 560 001, India

†*Corresponding Author Email: bmshankar@pes.edu*

ABSTRACT

The stability of buoyancy-driven parallel shear flow of a dielectric fluid confined between differentially heated vertical plates is investigated under the influence of a uniform horizontal AC electric field. The resulting generalized eigenvalue problem is solved numerically using Chebyshev collocation method with wave speed as the eigenvalue. The critical Grashof number G_c, the critical wave number α_c and the critical wave speed c_c are computed for wide ranges of AC electric Rayleigh number R_{ea} and the Prandtl number Pr. Based on these parameters, the stability characteristics of the system are discussed in detail. It is found that the AC electric Rayleigh number is to instill instability on convective flow against both stationary and travelling-wave mode disturbances. Nonetheless, the value of Prandtl number at which the transition from stationary to travelling-wave mode takes place is found to be independent of AC electric Rayleigh number. The streamlines and isotherms presented demonstrate the development of complex dynamics at the critical state.

NOMENCLATURE

a	vertical wave number		T_2	temperature of the right boundary
c	wave speed		V	root-mean-square value of the electric potential
c_r	phase velocity			
c_i	growth rate		V_1	electric potential of the left boundary
$D = d/dx$	differential operator			
$\vec{E}$	root-mean-square value of the electric field		V_2	electric potential of the right boundary
E_0	root-mean-square value of the electric field at $x = 0$		W_b	basic velocity
$\vec{f}_e$	force of electrical origin		(x, y, z)	Cartesian co-ordinates
$\vec{g}$	acceleration due to gravity		α	thermal expansion coefficient
G	Grashof number		γ	thermal expansion coefficient of dielectric constant
h	half- width of the dielectric fluid layer		ε	dielectric constant
p	pressure		ε_0	reference dielectric constant at T_0
P	modified pressure		κ	thermal diffusivity
Pr	Prandtl number		σ	electrical conductivity of the fluid
$\vec{q}$	velocity vector		μ	fluid viscosity
R_{ea}	AC electric Rayleigh number		ν	kinematic viscosity
t	time		ψ	stream function
T	temperature		Ψ	amplitude of vertical component of perturbed stream function
T_1	temperature of the left boundary			

ϕ	amplitude of perturbed electric potential	ρ_e	free charge density
		ρ_0	reference density at T_0
ρ	fluid density	θ	amplitude of perturbed temperature

1. INTRODUCTION

Hydrodynamic stability is one of the fundamental topics in fluid mechanics and the fluid flows in channels have been studied extensively (Chandrasekhar, 1981; Drazin and Reid, 2004). Fluid flows in many geophysical and astrophysical phenomena are maintained by buoyancy forces, but the role of these forces is generally strongly modified by co-existing shear, rotation of the system as a whole, processes at a free surface and so on. Natural convection of a viscous fluid in a vertical fluid layer, whose walls are held at different temperatures, provides one such simplest cases of an interaction between buoyancy and shearing forces. Instability of the base flow in such a fluid layer occurs when the Grashof number becomes greater than a certain critical value and the stability characteristics of the Newtonian fluid flow in the conduction regime are well established (Korpela *et al.*, 1973; Bergholz, 1978). The most interesting observation is that the type of instability is determined by the magnitude of the Prandtl number *Pr*. The critical disturbance modes are found to be stationary when $Pr < 12.7$, but they are travelling waves when $Pr > 12.7$. Vest and Arpaci (1969) studied the onset of stationary instability in the boundary-layer regime and reported fair agreement between their theoretical and experimental values for the critical Grashof number. Later on, using the power series method, Ruth (1979) obtained essentially exact values of the stability condition for $0.00001 < Pr < 10$.

A considerable number of theoretical and numerical studies on the stability of fluid flows have also been devoted to the interaction of electromagnetic fields with fluids. The stability of the flow of an electrically conducting fluid between parallel planes under a transverse magnetic field has been studied by Lock (1955), Potter and Kutchey (1973) and Takashima (1994, 1996) and showed that a transverse magnetic field has a powerful stabilizing influence on this type of flow. If the fluid is dielectric with low electrical conductivity then the electric forces play a major role rather than magnetic forces in driving the motion.

Electrohydrodynamic (EHD) stability of channel flow has attracted much attention, particularly because of its use in the field of micro fluidics. For instance, in many micro-electro-mechanical-systems (MEMS) devices, rapid mixing is highly desired and can be achieved by applying an electric field, as discussed in the experiments of Moctar *et al.* (2003), Glasgow *et al.* (2004) and Lin *et al.* (2004). A brief discussion on the applications of EHD instability has been presented by Lin (2009). The stability of a plane convective flow of dielectric fluid in a vertical layer has been investigated by Takashima and Hamabata (1984). They found that a

transition from stationary to travelling-wave instability occurs at a certain value of *Pr* between 12.4 and 12.5 which was later supported by Chen and Pearlstein (1989). Fujimura (1990) showed that the transition value of *Pr* is given by 12.45425644. Smorodin (2001) investigated the instability of convective liquid dielectric flow in the alternating field of a vertical capacitor with boundaries heated to different temperatures. EHD instability of an inviscid fluid in the presence of an electric field and space variation of electrical conductivity is studied by Shubha *et al.* (2008). Rudraiah *et al.* (2011) investigated EHD stability of couple stress fluid flow in a horizontal channel occupied by a porous medium using energy method. The effect of vertical AC/DC electric field on electrothermal convection has been discussed extensively (Turnbull, 1969; Stiles *et al.*, 1993; Shivakumara *et al.*, 2007, 2012, 2013, Rana *et al.*, 2015; Chand *et al.*, 2015; Chand 2015).

Heat transfer by means of thermal convection may not meet the requirements in most of the practical situations particularly in MEMS. In such circumstances, EHD enhanced heat transfer emerges as an important alternative method to enhance heat transfer. The intent of the present paper is to investigate the stability of natural convection in a vertical dielectric fluid layer under the influence of horizontal AC electric field. The vertical plates are maintained at constant but different temperatures and the normal electric field is held constant on the plates and as a result there exists variation in the dielectric constant which eventually causes electro-thermo-hydrodynamic instability by the dielectrophoretic force acting in the bulk of the fluid. The resulting eigenvalue problem is solved numerically using the Chebyshev collocation method and the existing results in the literature are obtained as limiting cases from the present study.

2. PROBLEM FORMULATION AND THE BASIC STATE

The physical configuration is as shown in Fig.1. We consider an incompressible dielectric fluid of thickness $2h$ confined between two parallel vertical plates at $x = \pm h$, subject to a uniform AC electric field applied across the layer; the left surface is maintained at fixed temperature T_1 and fixed electric potential $V_1(=0)$, whereas the plate at $x = h$ is maintained at fixed temperature $T_2(>T_1)$ and at an alternating (60 Hz) potential whose root-mean-square value is V_2. A Cartesian coordinate system (x, y, z) is chosen with the origin in the middle of the vertical fluid layer, where the x-axis is taken perpendicular to the plates and the

z-axis is vertically upwards, opposite in direction to the gravity. The relevant basic equations under the Oberbeck-Boussinesq approximation are (Chandrasekar, 1981; Shivakumara *et al.*, 2007):

$$\nabla \cdot \vec{q} = 0 \tag{1}$$

$$\rho_0 \left[\frac{\partial \vec{q}}{\partial t} + (\vec{q} \cdot \nabla) \vec{q} \right] = -\nabla p + \rho \vec{g} + \mu \nabla^2 \vec{q} + \vec{f}_e \tag{2}$$

$$\frac{\partial T}{\partial t} + (\vec{q} \cdot \nabla) T = \kappa \nabla^2 T \tag{3}$$
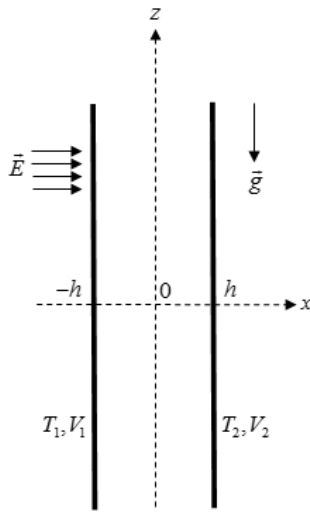
$$\rho = \rho_0 \{ 1 - \alpha (T - T_0) \} \tag{4}$$

Fig. 1. Physical configuration.

where $\vec{q} = (u, v, w)$ the velocity vector, T the temperature, p the pressure, ρ the fluid density, κ the thermal diffusivity, μ the fluid viscosity, $\vec{g}$ the acceleration due to gravity, α the thermal expansion coefficient, ρ_0 the density at reference temperature $T = T_0$, and $\vec{f}_e$ the force of electrical origin which can be expressed as (Landau and Lifshitz, 1960)

$$\vec{f}_e = \rho_e \vec{E} - \frac{1}{2} (\vec{E} \cdot \vec{E}) \nabla \varepsilon + \frac{1}{2} \nabla \left(\rho \frac{\partial \varepsilon}{\partial \rho} \vec{E} \cdot \vec{E} \right). \tag{5}$$

Here $\vec{E}$ is the root-mean-square value of the electric field, ρ_e is the free charge density and ε is the dielectric constant. The electrical force $\vec{f}_e$ will have no effect on the bulk of the dielectric fluid if the dielectric constant ε and the electrical conductivity σ are homogeneous. Since ε and σ are functions of temperature, a temperature gradient applied to a dielectric fluid produces a gradient in ε and σ. The application of DC electric field then results in the accumulation of free charge in the liquid. The free charge increases exponentially in time with a time constant ε/σ, which is known as the electrical relaxation time. If an AC electric field is applied at a frequency much higher than the

reciprocal of the electrical relaxation time, the free charge does not have time to accumulate. Moreover, the electrical relaxation time of most dielectric liquids appear to be sufficiently long to prevent the buildup of free charge at standard power line frequencies. At the same time, dielectric loss at these frequencies is so low that it makes no significant contribution to the temperature field. The Coulomb force term $\rho_e \vec{E}$ in Eq. (5) is the force per unit volume on a medium containing free electric charge of density ρ_e. It is the strongest EHD force term and usually dominates when DC electric fields are present in dielectric fluids. The second term in Eq. (5), called dielectrophoretic force term, is due to the force exerted on a dielectric fluid by a non-uniform electric field. It is usually weaker than the free charge force term and only dominates when an AC electric field is imposed on a dielectric fluid. Therefore, the Coulomb force term has been neglected in Eq. (5) and only the dielectrophoretic force term is retained in Eq. (5). It is seen that the dielectrophoretic force term depends on ($\vec{E} \cdot \vec{E}$) rather than $\vec{E}$. Since the variation of $\vec{E}$ is very rapid, the root-mean-square value of $\vec{E}$ is used as the effective value in determining fluid motion. In other words, one can treat the AC electric field as the DC electric field whose strength is equal to the root-mean-square value of the AC electric field (Takashima and Aldridge, 1976). The last term in Eq. (5) is called the electrostriction term. This term can be conveniently clubbed with the pressure in Eq. (5) and, because pressure amounts to an extra variable in incompressible flow, seems not to have any influence on the hydrodynamics.

Since there is no free charge, the relevant Maxwell equations are

$$\nabla \times \vec{E} = 0 \text{ or } \vec{E} = -\nabla V , \ \nabla \cdot (\varepsilon \vec{E}) = 0 . \tag{6a,b}$$

where V the root-mean-square value of the electric potential. The dielectric constant is assumed to be a linear function of temperature in the form $\varepsilon = \varepsilon_0 [1 - \gamma (T - T_0)]$, where γ (>0) the thermal expansion coefficient of dielectric constant and is assumed to be small. For example, for 10 cs Silicone oil $\gamma = 2.86 \times 10^{-3} K^{-1}$ and $\varepsilon = 2.6 \times 10^{-11} Fm^{-1}$. The basic state is given by

$$W_b = \frac{\alpha g \beta}{12 \nu} \left(h^2 - x^2 \right) x ,$$

$$P_b = \text{const} - \rho_0 g z + \frac{\varepsilon_0 E_0^2}{2(1 - \gamma \beta x)} ,$$

$$T_b - T_0 = b x / 2; b = DT / h , \rho_b = \rho_0 \left(1 - \frac{\alpha \beta x}{2} \right),$$

$$\varepsilon_b = \varepsilon_0 \left(1 - \frac{\gamma \beta x}{2} \right), \vec{E}_b = \frac{E_0}{1 - \gamma \beta x / 2} \hat{i} ,$$

$$V_b = \frac{2 E_0}{\gamma \beta} \log \left(\frac{1 - \gamma \beta x / 2}{1 + \gamma \beta h / 2} \right) \tag{7}$$

where $E_0 = (\gamma \beta V_2 / 2) \log[(1 + \gamma \beta h / 2)/(1 - \gamma \beta h / 2)]$ the root-mean-square value of the electric field at $x = 0$, $\nu(= \mu / \rho_0)$ the kinematic viscosity and $P = p - 0.5\rho(\partial \varepsilon / \partial \rho)(\vec{E} \cdot \vec{E})$ the modified pressure.

3. PERTURBED STATE AND THE LINEAR STABILITY EQUATIONS

To study the stability of the basic state, an infinitesimal disturbance on the base flow is superimposed in the form

$$\vec{q} = \vec{q}_b + \vec{q}', \quad P = P_b(x,z) + P', V = V_b + V',$$
$$T = T_b + T', \quad \rho = \rho_b + \rho', \quad \varepsilon = \varepsilon_b + \varepsilon'. \quad (8)$$
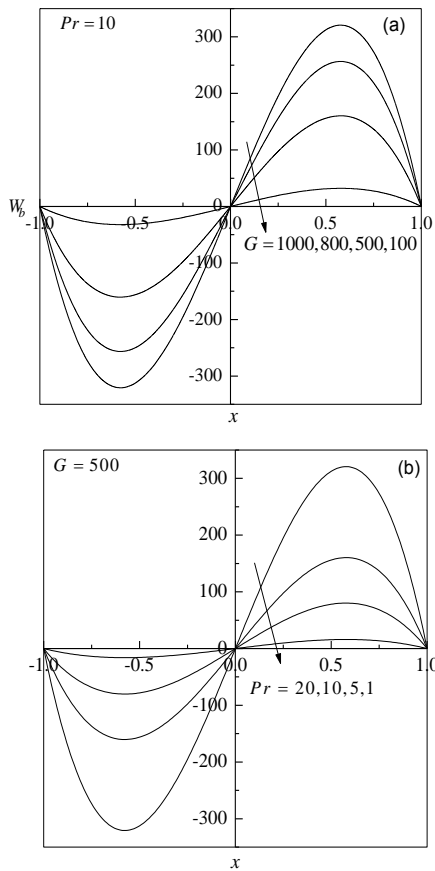

Fig. 2. Velocity profile W_b of the base flow for various values of (a) Grashof number G (b) Prandtl number Pr.

Substituting Eq.(8) into Eqs.(1)-(3), linearizing, eliminating the pressure from the momentum equation, introducing a stream function $\psi(x,z,t)$ through $u = \partial \psi / \partial z, w = -\partial \psi / \partial x$ and employing the normal mode analysis procedure in the form $\{\psi, T, V\} = \{\Psi, \theta, \phi\}(x)e^{ia(z-ct)}$, the stability equations in dimensionless form can then be shown to be

$$\left(\frac{W_b}{Pr} - c\right)(D^2 - a^2)\Psi - \frac{1}{Pr}D^2 W_b \Psi + \frac{R_{ea}}{2}(D\phi + \theta)$$
$$= \frac{1}{ia}\left[(D^2 - a^2)^2 \Psi - GPrD\theta\right] \quad (9)$$

$$\left(\frac{W_b}{Pr} - c\right)\theta + \frac{1}{2Pr}\Psi = \frac{1}{iaPr}(D^2 - a^2)\theta \quad (10)$$

$$D\theta + (D^2 - a^2)\phi = 0 \quad (11)$$

where $D = d/dx$, $R_{ea} = \gamma^2 \varepsilon_0 E_0^2 \beta^2 h^4 / \mu \kappa$ the AC electric Rayleigh number, $Pr = \nu / \kappa$ the Prandtl number, $G = \alpha g \beta h^4 / \nu^2$ the Grashof number, $c = c_r + ic_i$ is the wave speed and a is the vertical wave number. It should be noted here that the basic velocity in dimensionless form is $W_b = (GPr/12)(1-x^2)x$.

Equations (9) - (11) are to be solved subject to appropriate boundary conditions. Since the isothermal vertical plates are rigid and the normal electric field is held constant on the plates, the associated boundary conditions are

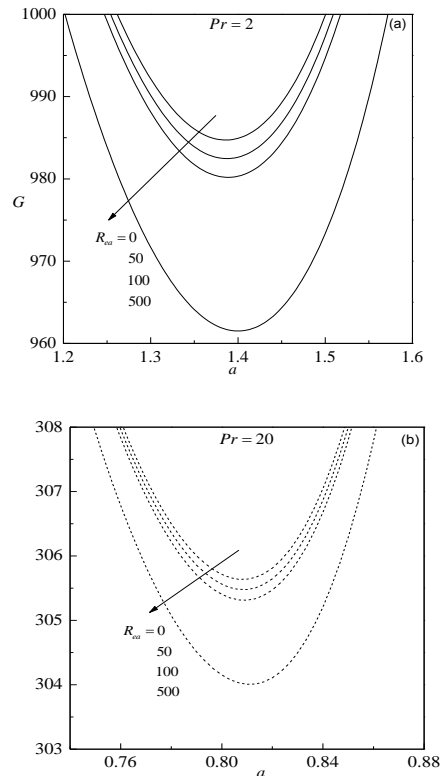$$\Psi = D\Psi = \theta = D\phi = 0 \text{ at } x = \pm 1. \quad (12)$$

Fig. 3. Neutral stability curves. Stationary modes (——) and travelling-wave modes (- - - -).

4. METHOD OF SOLUTION

Equations (9) - (11) together with the boundary

conditions (12) constitute an eigenvalue problem which has to be solved numerically. The resulting eigenvalue problem is solved using Chebyshev collocation method. The kth order Chebyshev polynomial and the Chebyshev collocation points are respectively given by $\xi_k(x) = \cos k\tau, \ \tau = \cos^{-1} x$ and

$x_j = \cos(\pi j / N), \ j = 0(1)N$. Here, the right and left wall boundaries correspond to $j = 0$ and N, respectively. The field variable Ψ, θ and ϕ can be approximated in terms of Chebyshev variable as follows

$$\Psi(x) = \sum_{j=0}^{N} \xi_n(x)\Psi_j, \ \theta(x) = \sum_{j=0}^{N} \xi_n(x)\theta_j,$$
$$\phi(x) = \sum_{j=0}^{N} \xi_n(x)\phi_j \tag{13}$$

The governing Eqs. (9) - (12) are discretized in terms of Chebyshev variable x to get

$$\left(\frac{W_b}{Pr} - c\right)\left(\sum_{k=0}^{N} B_{jk}\Psi_k - a^2\Psi_j\right) - \frac{1}{Pr}D^2 W_b \Psi_j$$
$$+ \frac{R_{ea}}{2}\left(\sum_{k=0}^{N} A_{jk}\phi_k + \theta_j\right)$$
$$= \frac{1}{ia}\left[\left(\sum_{k=0}^{N} C_{jk}\Psi_k + a^4\Psi_j - 2a^2\sum_{k=0}^{N} B_{jk}\Psi_k\right)\right] \tag{14}$$
$$- G\,Pr\sum_{k=0}^{N} A_{jk}\theta_k, j = 1(1)N-1$$

$$\left(\frac{W_b}{Pr} - c\right)\theta_j + \frac{1}{2Pr}\Psi_j$$
$$= \frac{1}{iaPr}\left(\sum_{k=0}^{N} B_{jk}\theta_k - a^2\theta_j\right), j = 1(1)N-1 \tag{15}$$
$$- G\,Pr\sum_{k=0}^{N} A_{jk}\theta_k, j = 1(1)N-1$$

$$\sum_{k=0}^{N} A_{jk}\theta_k + \left(\sum_{k=0}^{N} B_{jk}\phi_k - a^2\phi_j\right), j = 1(1)N-1 \tag{16}$$

$$\Psi_0 = \Psi_N = 0, \qquad \sum_{k=0}^{N} A_{jk}\Psi_k = 0, \ j = 0 \ \& \ N \quad ,$$

$$\theta_0 = \theta_N = 0, \ \sum_{k=0}^{N} A_{jk}\phi_k = 0, \ j = 0 \ \& \ N \tag{17}$$

where $A_{jk} = \begin{cases} \dfrac{c_j(-1)^{k+j}}{c_k(x_j - x_k)} & j \neq k \\[2ex] \dfrac{x_j}{2(1-x_j^2)} & 1 \leq j = k \leq N-1 \\[2ex] \dfrac{2N^2+1}{6} & j = k = 0 \\[2ex] -\dfrac{2N^2+1}{6} & j = k = N \end{cases}$,

$B_{jk} = A_{jm} \cdot A_{mk} \ \& \ C_{jk} = B_{jm} \cdot B_{mk}$.

with $c_j = \begin{cases} 2 & j = 0, N \\ 1 & 1 \leq j \leq N-1 \end{cases}$

The above equations form the system of linear algebraic equations

$$AX = cBX \tag{18}$$

where c is the eigenvalue and X is the discrete representation of the eigenfunction; A and B are square (complex) matrices of order $2(N+1)$. The eigenvalues and the eigenfunctions of the generalized eigenvalue problem (26) are determined with the aid of a QZ-algorithm which is available in the MATLAB software package in the form of built in function **eig( )**. The critical wave speed c_c, the corresponding critical Grashof number G_c and the wave number a_c are determined for various values of Prandtl number Pr and AC electric Rayleigh number R_{ea} following the procedure explained in Shankar *et al.* (2014a, b).

5. RESULTS AND DISCUSSION

The effect of uniform horizontal AC electric field on the stability of natural convection in a vertical dielectric fluid layer is investigated. The resulting eigenvalue problem is solved numerically using Chebyshev collocation method with wave speed as the eigenvalue. Critical Grashof number G_c and critical wave speed c_c are computed with respect to the wave number ' a 'for various values of AC electric Rayleigh number R_{ea} . In most of the experiments, the depth over which the electric permittivity varies with temperature is generally in the order of millimeters and the kinematic viscosity and thermal diffusivity of the water-borne liquid used for bio-fluidics are about $\nu = 9.7 \times 10^{-7} m^2/\sec$ and $\kappa = 1.4 \times 10^{-7} m^2/\sec$, respectively. Thus the Prandtl number is approximately 7, is used to examine the instability characteristics of the system.

Although the basic flow is independent of R_{ea}, it is significantly influenced by G and Pr. Figures 2(a) and (b) respectively show the influence of G and Pr on W_b. These figures indicate that decrease in G and Pr is to suppress the fluid flow. From the figures, it is also seen that, in general, the solution does not have symmetry with respect to x. This effect is due to the fixed direction of the gravitational field.

The convergence of the numerical method employed is tested by varying the order of base polynomial. Tables1 (a) and (b) illustrate the convergence of numerical solution for both stationary and travelling-wave mode cases for some selected values of parameters. To account for all the harmonics in a complicated solution, a large number of terms have to be included in the

Table 1 (a) Order of polynomial independency (stationary case)

N	$Pr=1, R_{ea}=100, G=800, a=2$		$Pr=1, R_{ea}=500, G=800, a=2$	
	c_i	c_r	c_i	c_r
5	-3.49104804	0	-2.81419066	0
10	-2.65629461	0	-2.35092099	0
15	-2.64890709	0	-2.35622640	0
20	-2.65888456	0	-2.35639837	0
25	-2.65893269	0	-2.35613876	0
30	-2.65893099	0	-2.35614144	0
35	-2.65893102	0	-2.35614382	0
40	-2.65893109	0	-2.35614417	0
45	-2.65893105	0	-2.35614419	0

Table 1 (b) Order of polynomial independency (oscillatory case)

N	$Pr=20, R_{ea}=100, G=200, a=0.8$		$Pr=20, R_{ea}=500, G=200, a=0.8$	
	c_i	c_r	c_i	c_r
5	-0.20306531	6.33035530	-0.20011071	6.33543156
10	-0.17430796	6.30451192	-0.17979262	6.34922163
15	-0.18753132	6.33482913	-0.18477346	6.33010841
20	-0.18768827	6.33510498	-0.18459924	6.32715172
25	-0.18778542	6.33599873	-0.18466634	6.32961864
30	-0.18779243	6.33510042	-0.18464876	6.32964395
35	-0.18779445	6.33511071	-0.18465482	6.32969732
40	-0.18779572	6.33511043	-0.18465897	6.32969198
45	-0.18779539	6.33511047	-0.18465829	6.32969186
50	-0.18779535	6.33511045	-0.18465823	6.32969181
55	-0.18779532	6.33511045	-0.18465825	6.32969180

Table 2 Comparison of critical stability parameters

R_{ea}	Pr	Chebyshev collocation method			Galerkin method		
		G_c	a_c	c_c	G_c	a_c	c_c
0	1	992.52946472	1.404	0	992.05636850	1.404	0
	5	982.99195862	1.384	0	982.51616156	1.384	0
	10	983.55348200	1.383	0	983.45694190	1.383	0
	15	487.16752625	0.608	$\pm$ 14.72510713	486.70350504	0.609	$\pm$ 14.69142688
	20	301.71983337	0.820	$\pm$ 9.29210134	301.16313195	0.823	$\pm$ 9.28312284
100	1	983.77495031	1.41	0	983.29598552	1.410	0
	5	981.16188049	1.384	0	980.68381047	1.385	0
	10	983.01658662	1.383	0	982.53865933	1.384	0
	15	486.97624251	0.608	$\pm$ 14.7190561	485.48028117	0.609	$\pm$ 14.68445735
	20	301.39884936	0.820	$\pm$ 9.28177151	300.82542396	0.820	$\pm$ 9.27498412
500	1	946.66938782	1.432	0	946.16446367	1.433	0
	5	973.74763489	1.390	0	973.26786558	1.391	0
	10	979.33311461	1.383	0	978.85510123	1.385	0
	15	486.13243103	0.609	$\pm$ 14.69075708	484.72027278	0.609	$\pm$ 14.66033584
	20	300.08049011	0.825	$\pm$ 9.23496285	299.54003489	0.823	$\pm$ 9.22083842

expansion. We have chosen different orders of Chebyshev polynomials and four digits point accuracy is achieved by retaining 30 terms in Eq. (13). As the number of terms increases in Eq. (13),

Table 3 The effect of R_{ea} on the values of Pr, G_c, a_c and c_c

R_{ea}	Pr	G_c	a_c	c_c
0	1	992.52946472	1.404	0
	5	982.99195862	1.384	0
	10	983.55348200	1.383	0
	12.6	984.09135449	1.383	0
	12.7	984.09135447	1.383	0
	12.8	831.82237442	0.400	± 24.830077
	13	769.99223337	0.420	± 23.041856
	15	487.16752634	0.607	± 14.725107
	20	301.71983348	0.820	± 9.292101
300	1	965.66581734	1.420	0
	5	977.47001656	1.387	0
	10	981.17637632	1.384	0
	12.6	981.93626478	1.383	0
	12.7	981.9576263	1.383	0
	12.8	831.1519623	0.397	± 24.824203
	13	769.1402435	0.424	± 23.001328
	15	486.5932465	0.607	± 14.708759
	20	300.7320404	0.821	± 9.259499
500	1	946.66938782	1.432	0
	5	973.74763489	1.390	0
	10	979.33311461	1.383	0
	12.6	980.4698944	1.386	0
	12.7	980.5019379	1.385	0
	12.8	830.8589935	0.397	± 24.815596
	13	768.9434052	0.424	± 22.995294
	15	486.13243103	0.609	± 14.690757
	20	300.08049011	0.825	± 9.234962

the results found to remain consistent and accuracy improved up to 7 digits for $N=40$ and $N=50$, respectively for stationary and travelling-wave mode cases. Thus more number of terms in Eq. (13) is required for convergence if the instability is via travelling-wave mode. By rigorous computational analysis, it was found that accurate solutions up to 8 digits could be reached by taking 60 terms in the Chebyshev collocation method and so for all further studies N is fixed at 60. To know the accuracy of the method employed to extract the stability parameters, the results are also obtained using Galerkin method (see Appendix A) with Legendre polynomials as trial functions for a representative set of parametric values and compared in Table 2. From the Table it is seen that the results are in good agreement.In Table 3, the values of G_c, a_c and c_c are tabulated for different values of R_{ea} and Pr ranging from 1 to 20 as the magnitude of Pr determines the mode of instability. The results for $R_{ea}=0$ correspond to an ordinary viscous fluid. It is observed that the critical disturbance modes are stationary when $Pr<12.7$ and they are travelling waves when $Pr>12.7$; a well-established result in the literature (Korpela *et al.*, 1973; Bergholz, 1978).

Interestingly the value of Prandtl number at which transition from stationary to travelling-wave instability occurs remain invariant for all values of R_{ea} considered. Nonetheless, the values of critical stability parameters vary with R_{ea}. The neutral stability curves in the (G,a) - plane are displayed in Figs. 3(a) and (b) for different values of R_{ea} for $Pr=2$ and 20, respectively. The neutral stability curves exhibit single but different minimum with respect to the wave number for various values of R_{ea} and Pr. The portion below each neutral curve corresponds to stable region and the region above corresponds to instability. It may be noted that, increase in R_{ea} and Pr leads to decrease the region of stability.

Figures 4(a) and (b) illustrate the variation of G_c and the corresponding a_c as a function of Pr for different values of R_{ea}. For a fixed value of R_{ea}, it is observed that the dependence of G_c upon Pr is very weak till $Pr<12.7$ and exceeding which G_c decreases suddenly. In other words, the Prandtl number shows no significant effect if the
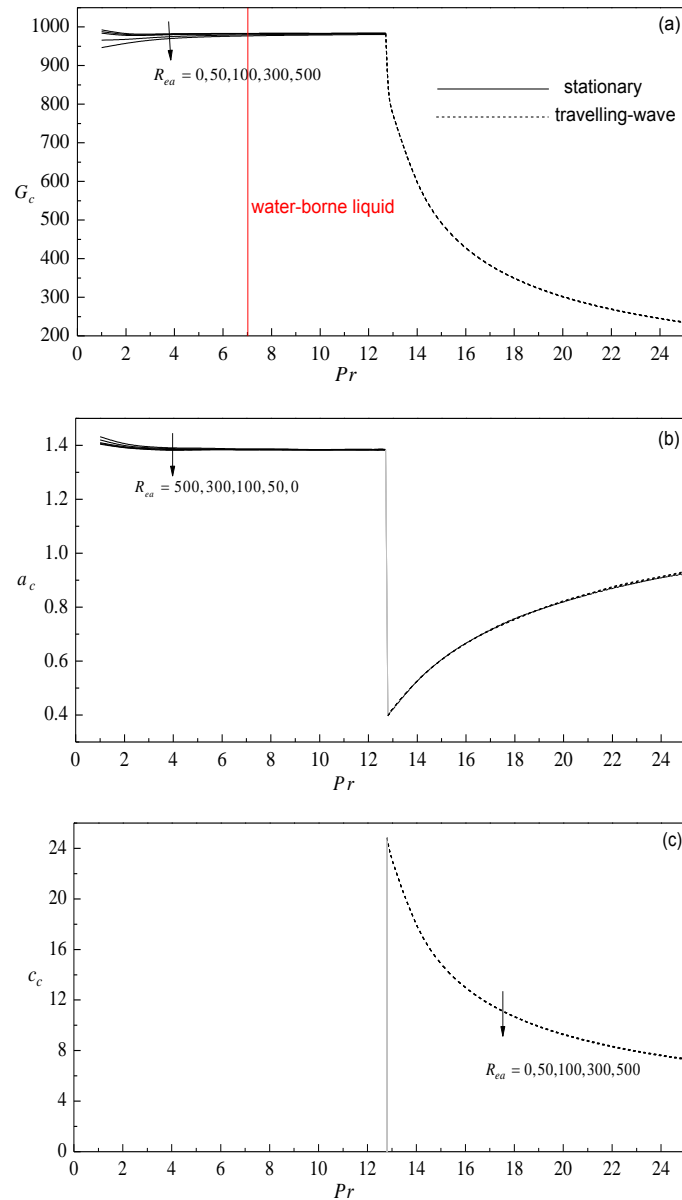
Fig. 4. Variation of (a) critical Grashof number G_c, (b) critical wave number a_c and (c) critical wave speed c_c with the Prandtl number Pr for various values of AC electric Rayleigh number R_{ea}.

disturbances are stationary, while its effect is significant if the disturbances are via travelling-wave modes. This may be due to the fact that the energy for stationary instability at low to moderate Pr is derived mainly from the base flow velocity field through the action of disturbance Reynolds stresses at the mid-plane between the upward and the downward flowing convective streams. Although the effect of increasing AC electric Rayleigh number is to instill instability on the system, its effect is found to be not so significant. If the disturbances are stationary, the critical wave number decreases slowly with increasing Pr while an opposite kind of behavior is noticed when the disturbances are travelling-wave modes (Fig. 4b). This is so for a fixed value of R_{ea}. Besides, the

critical wave number increases with increasing R_{ea} only at lower values of Pr. Further inspection of the figure reveals that, through the transition, the wave number drops from 1.4 to 0.4 and then increases again for higher values of Pr. This indicates two different physical mechanisms of instability. As Pr increases, there is a tendency for more of the disturbance energy to originate from the potential energy associated with the buoyancy effect than as transfer from the kinetic energy of the base flow by the action of Reynolds stresses.

The results regarding the nature of the travelling - wave instability summarized in Fig 5(c), indeed confirm this, which shows the variation of positive c_c with Pr for various values of R_{ea}. The vertical
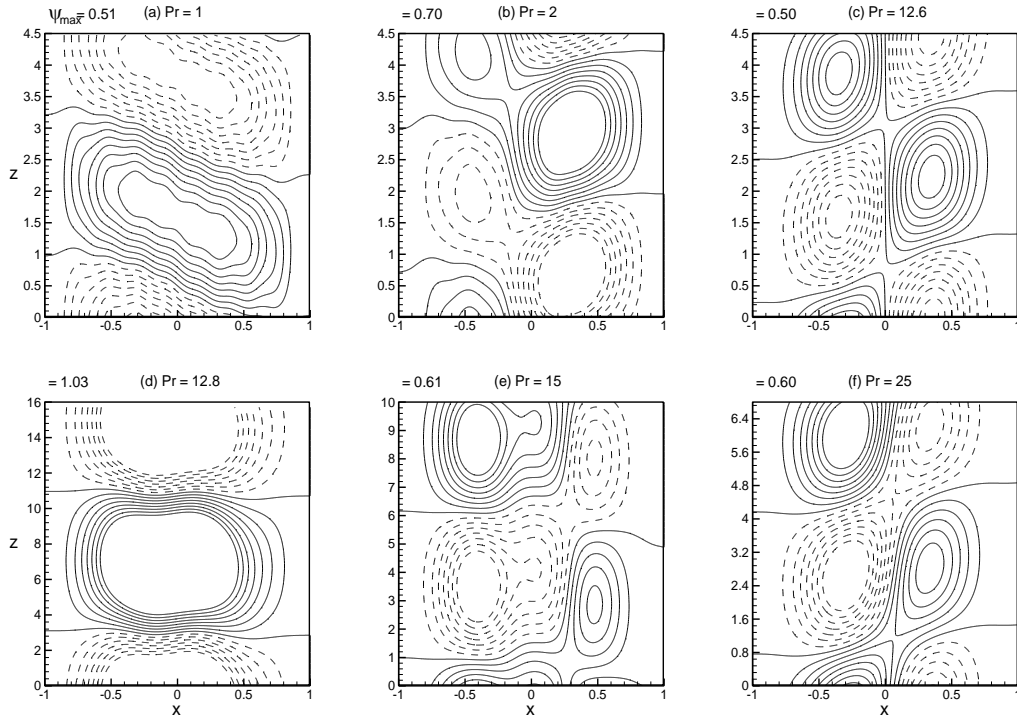
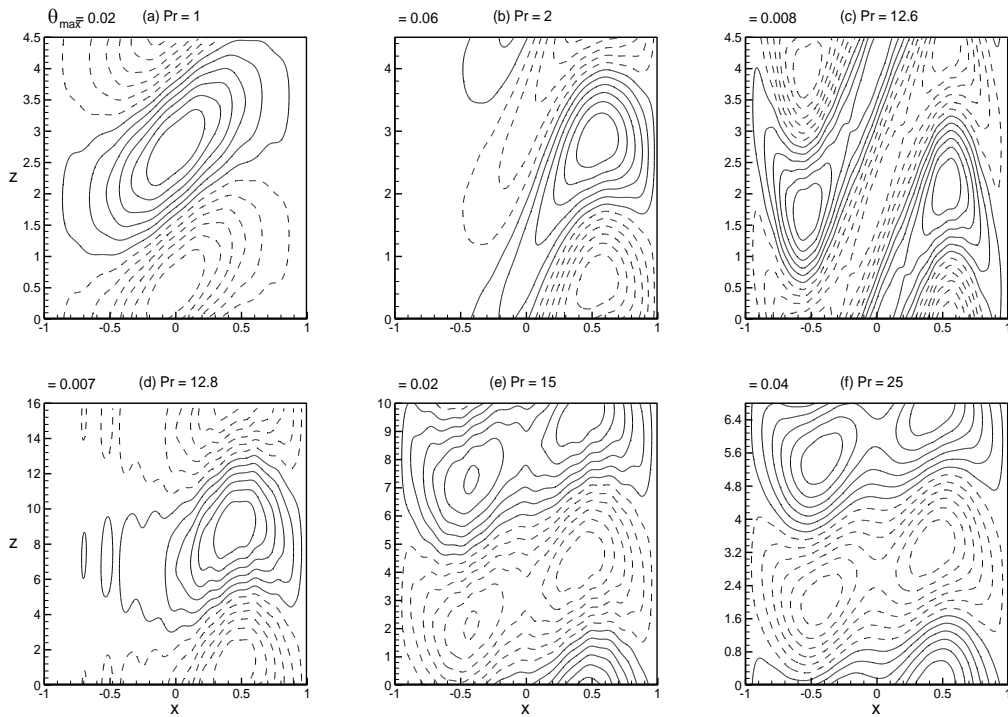**Fig. 5. Streamlines at $R_{ea} = 0$ for different values of Pr .**

Fig. 6. Isotherms at $R_{ea} = 0$ for different values of Pr .

lines represent the discontinuous changes in c_c due to the transition from stationary to travelling – wave mode. From the figure it is observed that c_c for the travelling – wave mode is a monotonically decreasing function of Pr . But the variation of R_{ea} on c_c is found to be insignificant.
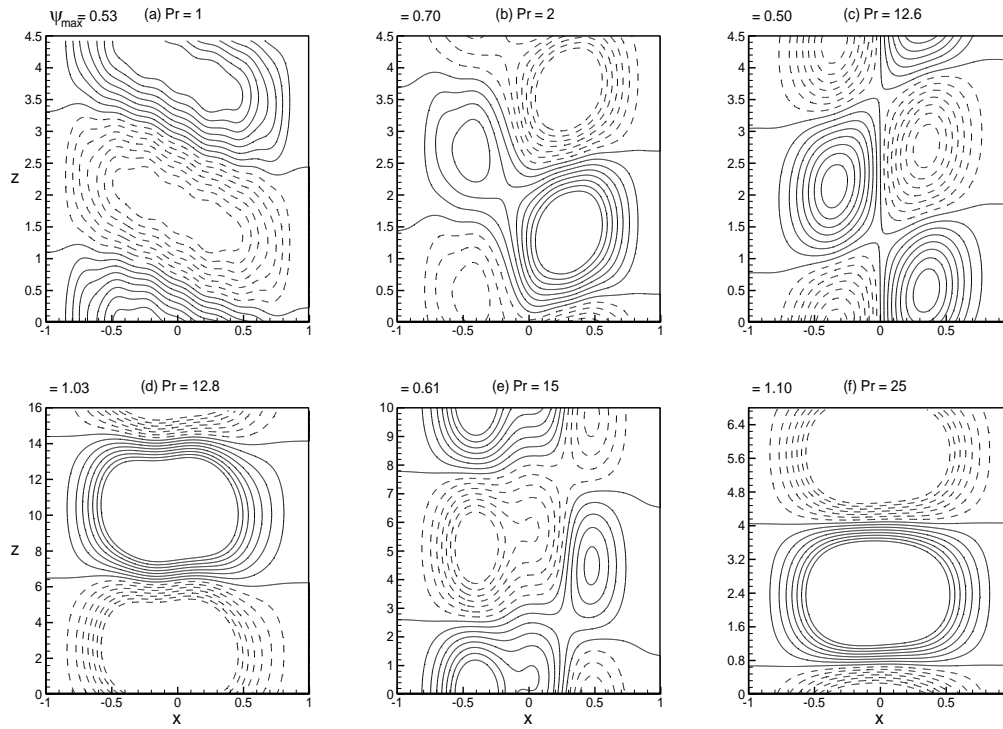
To know the influence of Pr and R_{ea} on the

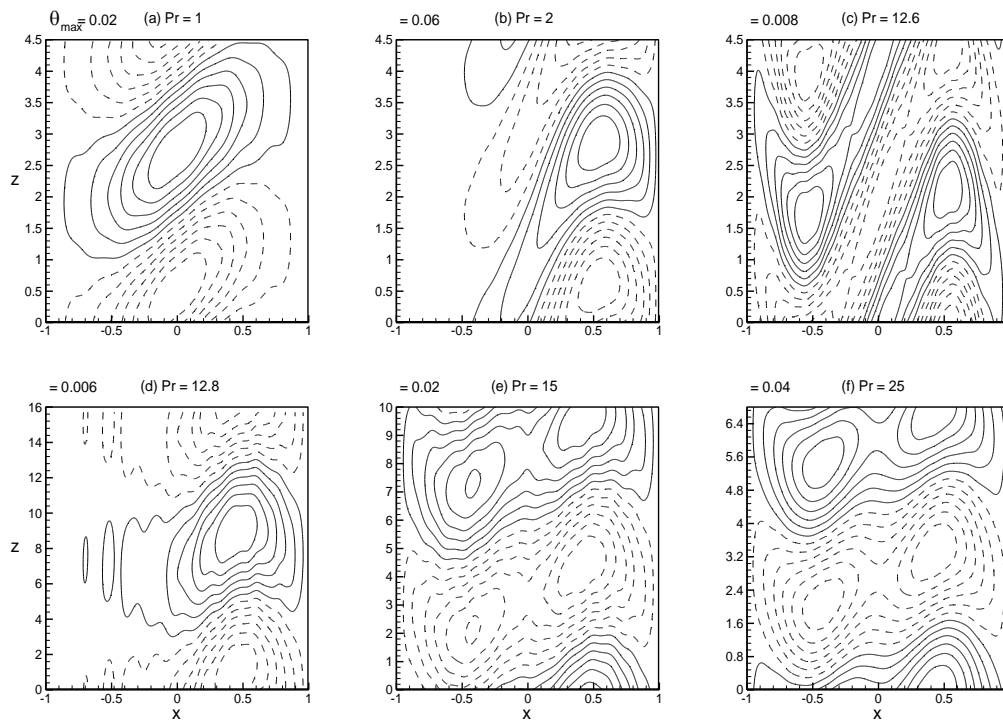**Fig. 7. Streamlines at $R_{ea} = 300$ for different values of Pr.**

Fig. 8. Isotherms for $R_{ea} = 300$ for different values of Pr.

disturbance flow and temperature, the corresponding streamlines and isotherms (Shankar *et al.* 2015, 2016) at the critical state for both stationary and travelling-wave modes are displayed in Figs. 5-10 for different values of Pr and R_{ea}.

Figures 5 and 6 show the results for R_{ea} =0 (i.e. ordinary viscous fluids) for different values of Pr. For Pr =1, the flow pattern appears to be stationary cellular convection with an inclination in streamlines and isotherms as shown in Figs. 5(a)
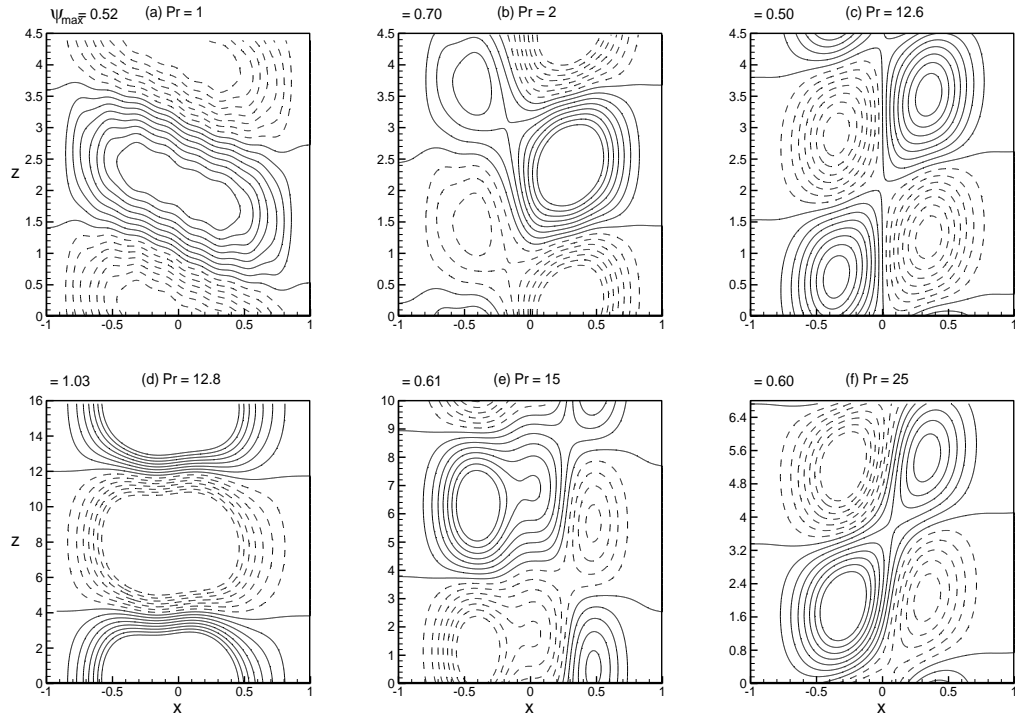
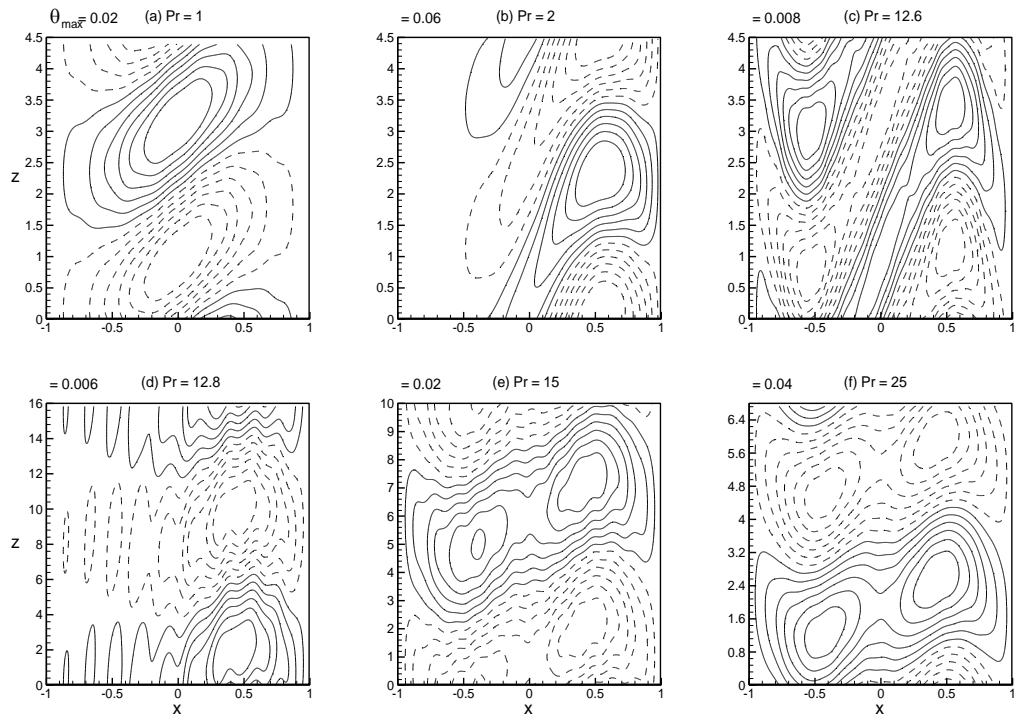**Fig. 9. Streamlines at $R_{ea} = 500$ for different values of Pr.**

Fig. 10. Isotherms at $R_{ea} = 500$ for different values of Pr.

and 6(a), respectively.

Further increase in Pr (= 2 and 12.6) results to force the convective motion to move closer and become parallel at the center of the fluid layer and also convective cells become uni-cellular to bi-

cellular. This fact is evident from Figs. 5(b) and (c). For $Pr = 2$, the isotherms concentrate in the vicinity of the hot wall (Fig. 6b) and become bi-cellular oblate triangles which are occupying almost the whole thickness of vertical fluid layer for $Pr = 12.6$

(Fig. 6c). However, the strength of secondary flow for the streamlines and isotherms do not vary much as a function of Pr in the stationary region. An flow strength changes qualitatively as well as quantitatively as the mode changes from stationary to travelling-wave mode. In other words, the instability switches over from stationary to travelling-wave mode once the value of Pr exceeds 12.7. When $Pr = 12.8$, convective cells become bi-cellular to uni-cellular in streamlines. Also, shape of the isotherms changes from bi-cellular oblate triangles to uni-cellular oblate triangles and concentrates in the vicinity of the hot wall. It is further seen that the actual wavelength substantially larger in both streamlines and isotherms and at this stage ψ_{max} increases from 0.50 to 1.03. This fact is evident from Figs. 5(d) and 6(d). Further increase in Pr is seen to decrease the flow strength (Figs. 5e and f) and also to weaken the isotherms (Figs. 6e and f). Interestingly, secondary flow behavior remains invariant for all values of AC electric Rayleigh number considered. The streamlines and isotherms illustrated in Figs. 7-10 for two values of $R_{ea} = 300$ and 500 also corroborate this behavior.

6. CONCLUSIONS

From the foregoing study, it is observed that a uniform AC electric field has no influence on the basic velocity distribution. The instability sets in as stationary convection with critical Grashof number G_c nearly independent of Pr for values of $Pr < 12.7$. The wave length of the critical disturbances is slightly larger than twice the separation of the vertical plates. For $Pr > 12.7$ the instability sets in as a wave travelling in the vertical direction with a wave speed which is first less than the maximum base flow velocity but decreases with increasing Pr. For Pr close to 12.8 the wavelength of the critical wave is nearly 8 times the width between the plates. Finally, as the Pr increased, the instability becomes more thermal in its origin. Moreover, the value of Pr at which transition from stationary to travelling-wave mode instability occurs remain invariant for all values of AC electric Rayleigh number. The effect of increasing AC electric Rayleigh number is to instill instability on the system but its effect is found to be not so significant. The streamlines and isotherms are found to mimic the behavior of stability curves observed before and after the change of mode of instability. Besides, a sudden change in streamlines and isotherms is observed both in their magnitude and pattern just before and after the transition mode. For the range of parametric values considered, convective cells found to appear both in bi-cellular as well as uni-cellular in nature.

ACKNOWLEDGEMENTS

REFERENCES

Bergholz, R. F. (1978). Instability of steady natural convection in a vertical fluid layer. *Journal of Fluid Mechanics* 84, 743-768.

Chand, R. (2015). Electro-thermal convection in a Brinkman porous medium saturated by

nanofluid. *Ain Shams Engineering Journal*.

Chand, R., Y. Dhananjaya and G. C. Rana (2015). Electrothermo convection in a horizontal layer of rotating nanofluid. *International Journal of Nanoparticles* 8, 241-261.

Chandrasekhar, S. (1981). *Hydrodynamic and Hydromagnetic Stability*, Dover, New York.

Chen, Y. M. and A. J. Pearlstein (1989). Stability of free-convection flows of variable viscosity fluids in vertical and inclined slots. *Journal of Fluid Mechanics* 198, 513-541.

Drazin, P. G. and W. H. Reid (2004). *Hydrodynamic Stability. Cambridge*, Cambridge University Press, UK.

El Moctar, A. O., N. Aubry and J. Batton (2003). Electrohydrodynamic micro-fluidic mixer. *Lab Chip* 3, 273–280.

Fujimura, K. (1990). Automated finder for the critical condition on the linear stability of fluid motions. *JAERI-M* 90-057.

Glasgow, I., J. Batton and N. Aubry (2004). Electroosmotic mixing in microchannels. *Lab Chip* 4, 558-562.

Korpela, S. A., D. Gozum and C. B. Baxi (1973). On the stability of the conduction regime of natural convection in a vertical slot. *International Journal of Heat and Mass Transfer* 16, 1683-1690.

Landau, L. D. and E. M. Lifshitz (1960). Electrodynamics of Continuous Media, Pergamon Press.

Lin, H. (2009). Electrokinetic instability in microchannel flows: A review. *Mechanics Research Communications* 36, 33-38.

Lin, H., B. D. Storey, M. H. Oddy, C. H. Chen and J. G. Santiago (2004). Instability of electrokinetic microchannel flows with conductivity gradients. *Physics of Fluids* 16, 1922–1935.

Lock, R. C. (1955). The stability of the flow of an electrically conducting fluid between parallel planes under a transverse magnetic field. In *Proceedings of Royal Society London A* 233,

105–125.

Potter, M. C. and J. A. Kutchey (1973). Stability of plane Hartmann flow subject to a transverse magnetic field. *Physics of Fluids* 16, 1848-1851.

Rana, G. C., R. Chand and D. Yadav (2015). The onset of electrohydrodynamic instability of an elastico-viscous Walters' (model B') dielectric fluid layer. *FME Transactions* 43, 154-160.

Rudraiah, N., B. M. Shankar and C. O. Ng (2011). Electrohydrodynamic stability of couple stress fluid flow in a channel occupied by a porous medium. *Special Topics and Reviews in Porous Media* 2, 11-22.

Ruth, D. W. (1979). On the transition to transverse rolls in an infinite vertical fluid layer a power series solution. *International Journal of Heat and Mass Transfer* 22, 1199-1208.

Shankar, B. M., Jai Kumar and I. S. Shivakumara (2014). Stability of natural convection in a vertical couple stress fluid layer. *International Journal of Heat and Mass Transfer* 78, 447–459

Shankar, B. M., Jai Kumar and I. S. Shivakumara (2015). Effect of horizontal alternating current electric field on the stability of natural convection in a dielectric fluid saturated vertical porous layer. *Journal of Heat Transfer* 137, 042501-1-9.

Shankar, B. M., Jai Kumar and I. S. Shivakumara (2016). Stability of natural convection in a vertical dielectric couple stress fluid layer in the presence of a horizontal ac electric field. *Applied Mathematical Modelling*, 40, 5462-5481.

Shankar, B. M., Jai Kumar, I. S. Shivakumara and C. O. Ng (2014b). Stability of fluid flow in a Brinkman porous medium A numerical study*. *Journal of Hydrodynamics* 26, 681-688.

Shivakumara, I. S., Jinho Lee, K. Vajravelu and M. Akkanagamma (2012). Electrothermal convection in a rotating dielectric fluid layer: Effect of velocity and temperature boundary conditions. *International Journal of Heat and Mass Transfer* 55, 2984-2991.

Shivakumara, I. S., M. Akkanagamma and C.O. Ng (2013). Electrohydrodynamic instability of a rotating couple stress dielectric fluid layer. *International Journal of Heat and Mass Transfer* 62, 761-771.

Shivakumara, I. S., M. S. Nagashree and K. Hemalatha (2007). Electrothermoconvective instability in a heat generating dielectric fluid layer. *International Communication in Heat and Mass Transfer* 34, 1041-1047.

Shubha, N., N. Rudraiah and K. W. Chow (2008). Electrohydrodynamic stability of poorly conducting parallel fluid flow in the presence of transverse electric field. *International Journal of Non-Linear Mechanics* 43, 643–649.

Smorodin, B. L. (2001). Stability of plane flow of a liquid dielectric in a transverse alternating electric field. *Fluid Dynamics* 36, 548–555.

Stiles, P. J., F. Lin and P. J. Blennerhassett (1993). Convective heat transfer through polarized dielectric liquids. *Physics of Fluids A* 5, 3273-3279.

Takashima, M. (1994). The stability of natural convection in a vertical layer of electrically conducting fluid in the presence of a transverse magnetic fluid. *Fluid Dynamics Research* 14, 121-134.

Takashima, M. (1996). The stability of the modified plane Poiseuille flow in the presence of a transverse magnetic field. *Fluid Dynamics Research* 17, 293-310.

Takashima, M. and H. Hamabata (1984). The stability of natural convection in a vertical layer of dielectric fluid in the presence of a horizontal ac electric field. *Journal of the Physical Society of Japan* 53, 1728-1736.

Takashima, M. and K. D. Aldridge (1976). The stability of a horizontal layer of dielectric fluid under the simultaneous action of a vertical dc electric field and a vertical temperature gradient. *The Quarterly Journal of Mechanics and Applied Mathematics* 29, 71-87.

Turnbull, R. J. (1969). Effect of dielectrophoretic forces on the Benard instability. *Physics of Fluids* 12, 1809-1815.

Vest, C. M. and V. S. Arpaci (1969). Stability of natural convection in a vertical slot. *Journal of Fluid Mechanics* 36, 1-15.

Appendix A

The resulting eigenvalue problem is solved using a simple but powerful Galerkin method. Accordingly, $\Psi(x)$, $\theta(x)$ and $\phi(x)$ are expanded in terms of Legendre polynomials in the form

$$\Psi(x) = \sum_{n=1}^{N} a_n \xi_n(x), \theta(x) = \sum_{n=1}^{N} a_n \zeta_n(x),$$

$$\phi(x) = \sum_{n=1}^{N} a_n \varsigma_n(x) \tag{A1}$$

with the corresponding base functions

$$\xi_n(x) = \left(1-x^2\right)^2 P_n(x), \ \zeta_n(x) = \left(1-x^2\right) P_n(x),$$

$$\varsigma_n(x) = \begin{cases} \left(1-x^2\right) P_n(x) + 2P_1 & \text{for odd } n \\ \left(1-x^2\right) P_n(x) + \dfrac{2}{3}P_2 & \text{for even } n \end{cases} \tag{A2}$$

$P_n(x)$ is the Legendre polynomial of degree n and a_n are constants. It may be noted that $\Psi(x), \theta(x)$ and $\phi(x)$ satisfies the boundary conditions. Equation (A1) is substituted into Eqs.(9) - (12) and the resulting error is required to be orthogonal to

$\Psi_m(x), \theta_m(x), \phi_m(x)$ for $m = 1, 2, \ldots\ldots N$. This gives

$$Pr \sum_{n=0}^{N} a_n \int_{-1}^{1} \left(\xi_n'' \xi_m'' + 2\alpha^2 \xi_n' \xi_m' + \alpha^4 \xi_n \xi_m \right) dx$$

$$+ i\alpha \sum_{n=0}^{N} a_n \int_{-1}^{1} \left\{ \left(\frac{d^2 W_B}{dx^2} + \alpha^2 u_B \right) \xi_n \xi_m - W_B \xi_n'' \xi_m \right\} dx$$

$$- G Pr^2 \sum_{n=0}^{N} b_n \int_{-1}^{1} \zeta_n' \xi_m \, dx$$

$$- \frac{i\alpha Pr R_{ea}}{2} \left(\sum_{n=0}^{N} b_n \int_{-1}^{1} \left(\zeta_n \xi_m \right) dx + \sum_{n=0}^{N} c_n \int_{-1}^{1} \left(\varsigma_n' \xi_m \right) dx \right)$$

$$= i\alpha c \, Pr \sum_{n=0}^{N} a_n \int_{-1}^{1} \left(\xi_n' \xi_m' + \alpha^2 \xi_n \xi_m \right) dx \quad \text{(A3)}$$

$$\frac{i\alpha}{2} \sum_{n=0}^{N} a_n \int_{-1}^{1} \xi_n \zeta_m \, dx + i\alpha \sum_{n=0}^{N} b_n \int_{-1}^{1} W_B \, \zeta_n \zeta_m \, dx$$

$$+ \sum_{n=0}^{N} b_n \int_{-1}^{1} \left(\zeta_n' \zeta_m' + \alpha^2 \zeta_n \zeta_m \right) dx \quad \text{(A4)}$$

$$= i\alpha c \, Pr \sum_{n=0}^{N} b_n \int_{-1}^{1} \zeta_n \zeta_m \, dx$$

$$- \sum_{n=0}^{N} b_n \int_{-1}^{1} \left(\zeta_n' \varsigma_m \right) dx + \sum_{n=0}^{N} c_n \int_{-1}^{1} \left(\varsigma_n' \varsigma_m' + \alpha^2 \varsigma_n \varsigma_m \right) dx = 0$$

$$\text{(A5)}$$

in which the primed quantities denote differentiation with respect to x.